Star-in-a-box setup for late-type stars

Carolina Ortiz Rodríguez (Universität Hamburg, Germany)

Petri Käpylä (Leibniz-Institute for Solar Physics (KIS), Germany)
Felipe Navarrete (Institut d'Estudis Espacials de Catalunya (IEEC), Spain)
Dominik Schleicher (Universidad de Concepción, Chile)
Barbara Toro (Universidad de Concepción, Chile)
Juan Pablo Hidalgo (Universidad de Concepción, Chile)
Robi Banerjee (Universität Hamburg, Germany)

A&A 651, A66 (2021)
https://doi.org/10.1051/0004-6361/202040049

Astronomy & Astrophysics

Star-in-a-box simulations of fully convective stars

P. J. Käpylä[1,2]

[1] Georg-August-Universität Göttingen, Institut für Astrophysik, Friedrich-Hund-Platz 1, 37077 Göttingen, Germany
e-mail: pkaepyl@uni-goettingen.de
[2] Nordita, KTH Royal Institute of Technology and Stockholm University, 10691 Stockholm, Sweden

Received 2 December 2020 / Accepted 11 April 2021

ABSTRACT

Context. Main-sequence late-type stars with masses of less than 0.35 $M_\odot$ are fully convective.
Aims. The goal is to study convection, differential rotation, and dynamos as functions of rotation in fully convective stars.
Methods. Three-dimensional hydrodynamic and magnetohydrodynamic numerical simulations with a star-in-a-box model, in which a spherical star is immersed inside of a Cartesian cube, are used. The model corresponds to a 0.2 $M_\odot$ main-sequence M5 dwarf. A range of rotation periods ($P_{\rm rot}$) between 4.3 and 430 d is explored.
Results. The slowly rotating model with $P_{\rm rot}$ = 430 days produces anti-solar differential rotation with a slow equator and fast poles, along with predominantly axisymmetric quasi-steady large-scale magnetic fields. For intermediate rotation ($P_{\rm rot}$ = 144 and 43 days) the differential rotation is solar-like (fast equator, slow poles), and the large-scale magnetic fields are mostly axisymmetric and either quasi-stationary or cyclic. The latter occurs in a similar parameter regime as in other numerical studies in spherical shells, and the cycle period is similar to observed cycles in fully convective stars with rotation periods of roughly 100 days. In the rapid rotation regime the differential rotation is weak and the large-scale magnetic fields are increasingly non-axisymmetric with a dominating m = 1 mode. This large-scale non-axisymmetric field also exhibits azimuthal dynamo waves.
Conclusions. The results of the star-in-a-box models agree with simulations of partially convective late-type stars in spherical shells in that the transitions in differential rotation and dynamo regimes occur at similar rotational regimes in terms of the Coriolis (inverse Rossby) number. This similarity between partially and fully convective stars suggests that the processes generating differential rotation and large-scale magnetism are insensitive to the geometry of the star.

Key words. stars: magnetic field – dynamo – magnetohydrodynamics (MHD) – convection – turbulence

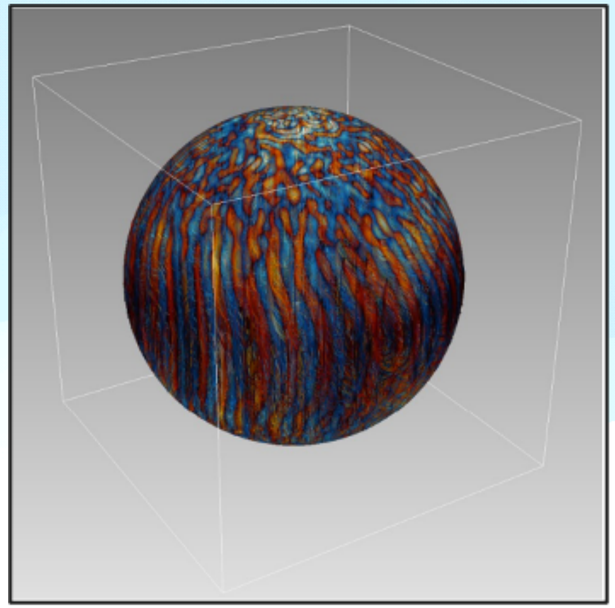

Credit: Petri Käpylä

First version by Dobler, W., Stix, M., & Brandenburg, A. (2006). *The Astrophysical Journal*, *638*(1), 336.

Star-in-a-box setup: set of equations

Käpylä, 2021, A&A, 651, A66

The non-ideal fully compressible MHD equations of induction, continuity, motion and energy conservation are solved with the Pencil Code:

$$\frac{\partial \boldsymbol{A}}{\partial t} = \boldsymbol{u} \times \boldsymbol{B} - \eta \mu_0 \boldsymbol{J}$$

$$\frac{\mathrm{D} \ln \rho}{\mathrm{D}t} = -\boldsymbol{\nabla} \cdot \boldsymbol{u}$$

$$\frac{\mathrm{D}\boldsymbol{u}}{\mathrm{D}t} = -\boldsymbol{\nabla}\Phi - \frac{1}{\rho}(\boldsymbol{\nabla} p - \boldsymbol{\nabla} \cdot 2\nu\rho\boldsymbol{S} + \boldsymbol{J} \times \boldsymbol{B}) - 2\boldsymbol{\Omega} \times \boldsymbol{u} + \boldsymbol{f}_d$$

$$T\frac{\mathrm{D}s}{\mathrm{D}t} = -\frac{1}{\rho}[\boldsymbol{\nabla} \cdot (\boldsymbol{F}_{\mathrm{rad}} + \boldsymbol{F}_{\mathrm{SGS}}) + \mathcal{H} - \mathcal{C}] + 2\nu\boldsymbol{S}^2 + \mu_0 \eta \boldsymbol{J}^2$$

Boundary conditions:

- Impenetrable and stress free for the flow

$$u_n = 0, \quad \partial \boldsymbol{u}_{\tan} = 0, \quad n = x, y, z.$$

- The magnetic field is assumed to be perpendicular to the boundary

$$\partial_n B_n = 0, \quad B_{\tan} = 0.$$

- Temperature is symmetric across the exterior boundaries of the box.
- Vanishing second derivative for the density.

Star-in-a-box setup: set of runs

Ortiz-Rodríguez et al. A&A 678, A82 (2023)

Fully convective setup at three different rotation rates,

$\tilde{\Omega} = 1.0, 0.7, 0.5$, which correspond to $P_{\rm rot} = 43, 60, 90$ days.

$\mathrm{Pr_M}$ was varied from 0.1 to 10.

Table 1. Simulation parameters.

Sim	$\tilde{\Omega}$	$\tilde{u}_{\rm rms}$	$B_{\rm rms}\,[B_{\rm eq}]$	$\mathrm{Pr_M}$	$\mathrm{Pr_{SGS}}$	$\mathrm{Re_M}$	Re	Co	Co_ω	Ta	Pe	Grid
A1	1.0	0.022	0.92	0.1	0.04	55	549	9.2	1.4	4.00×10^{10}	22	200^3
A2	1.0	0.021	0.94	0.1	0.04	79	788	9.3	1.2	8.30×10^{10}	32	288^3
A3	1.0	0.021	0.91	0.2	0.08	54	272	9.3	1.6	1.00×10^{10}	22	200^3
A4	1.0	0.022	0.81	0.5	0.20	54	109	9.3	1.9	1.60×10^{9}	22	200^3
A5	1.0	0.022	0.75	0.7	0.28	55	78	9.2	2.0	8.16×10^{8}	22	200^3
A6	1.0	0.020	0.91	0.7	0.28	75	107	9.7	2.0	1.69×10^{9}	30	200^3
A7	1.0	0.021	0.84	0.9	0.20	54	108	9.4	1.9	1.60×10^{9}	22	200^3
A8$^{(*)}$	1.0	0.030	–	0.2	0.28	22	108	6.6	1.8	8.16×10^{8}	30	200^3
A9	1.0	0.022	0.71	0.5	0.28	39	78	9.3	2.1	8.16×10^{8}	22	200^3
A10	1.0	0.020	0.89	1.0	0.20	105	105	9.7	1.9	1.60×10^{9}	21	200^3
A11	1.0	0.020	0.88	1.0	0.28	73	73	9.9	2.1	8.16×10^{8}	20	200^3
A12$^{(*)}$	1.0	0.028	–	1.0	0.40	70	70	7.2	2.0	4.00×10^{8}	28	200^3
A13	1.0	0.019	0.81	2.0	0.40	99	50	10.1	2.3	4.00×10^{8}	20	200^3
A14	1.0	0.017	1.20	5.0	0.40	208	42	12.1	2.4	4.00×10^{8}	17	200^3
A15	1.0	0.017	1.16	7.0	0.40	300	42	12.0	2.5	4.00×10^{8}	17	200^3
A16	1.0	0.016	1.24	10.0	0.40	390	39	12.9	2.5	4.00×10^{8}	16	200^3
B1	0.7	0.024	0.68	0.5	0.40	84	167	5.9	1.1	1.51×10^{9}	62	200^3
B2	0.7	0.024	0.74	1.0	0.40	168	168	5.8	1.0	1.51×10^{9}	68	576^3
B3	0.7	0.022	0.88	2	0.40	315	158	6.2	1.0	1.51×10^{9}	64	576^3
B4	0.7	0.020	1.03	5	0.40	714	143	6.9	1.1	1.51×10^{9}	58	576^3
B5	0.7	0.019	1.02	10	0.40	1360	135	7.2	1.2	1.51×10^{9}	55	576^3
C1	0.5	0.025	0.80	1.0	0.20	256	256	3.9	0.6	1.60×10^{9}	51	576^3
C2$^{(*)}$	0.5	0.032	–	0.5	0.40	41	21	3.1	0.9	1.00×10^{8}	32	200^3
C3	0.5	0.026	0.53	1.0	0.40	67	67	3.8	1.1	1.00×10^{8}	27	200^3
C4	0.5	0.024	0.85	2	0.40	337	168	4.1	0.7	7.71×10^{8}	68	576^3
C5	0.5	0.021	1.17	5	0.40	750	150	4.7	0.7	7.71×10^{8}	60	576^3
C6	0.5	0.020	1.02	10	0.40	1419	142	4.9	0.8	7.71×10^{8}	51	576^3

Notes. Summary of the simulations. From left to right the columns correspond to the following: Sim is the simulation name, $\tilde{\Omega} = \Omega\tau_{\rm ff}$ is the normalised rotation rate, $\tilde{u}_{\rm rms} = u_{\rm rms}/(GM/R)^{1/2}$ is the normalised root main square velocity, $B_{\rm rms}$ is the root main square magnetic field strength in units of the equipartition strength, $\mathrm{Pr_M}$ and $\mathrm{Pr_{SGS}}$ are the magnetic and subgrid-scale Prandtl numbers, $\mathrm{Re_M}$ and Re are the magnetic and fluid Reynolds numbers, Co and Co_ω are the global and local Coriolis numbers, Ta is the Taylor number, and Pe is the Péclet number. The last column indicates the grid resolution. $^{(*)}$ Runs with no dynamo.

Differential rotation

Ortiz-Rodríguez et al. A&A 678, A82 (2023)

Amplitude of the radial and latitudinal differential rotation

$$\Delta_{\Omega}^{(r)} = \frac{\overline{\Omega}_{\mathrm{top,eq}} - \overline{\Omega}_{\mathrm{bot,eq}}}{\overline{\Omega}_{\mathrm{top,eq}}}$$

$$\Delta_{\Omega}^{(\bar{\theta})} = \frac{\overline{\Omega}_{\mathrm{top,eq}} - \overline{\Omega}_{\mathrm{bot},\bar{\theta}}}{\overline{\Omega}_{\mathrm{top,eq}}}$$

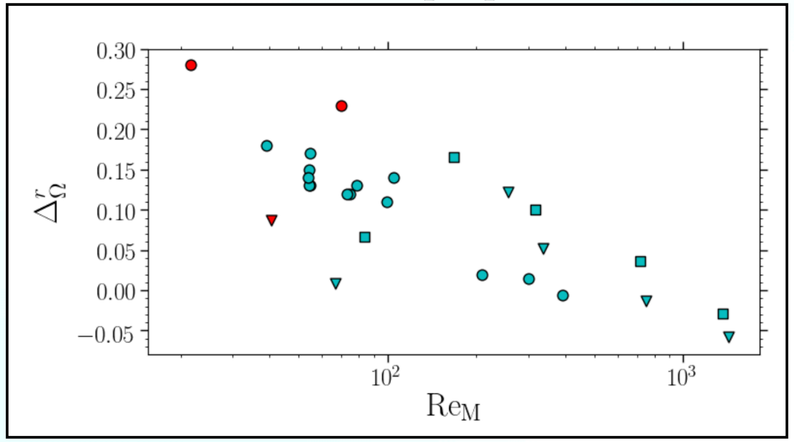

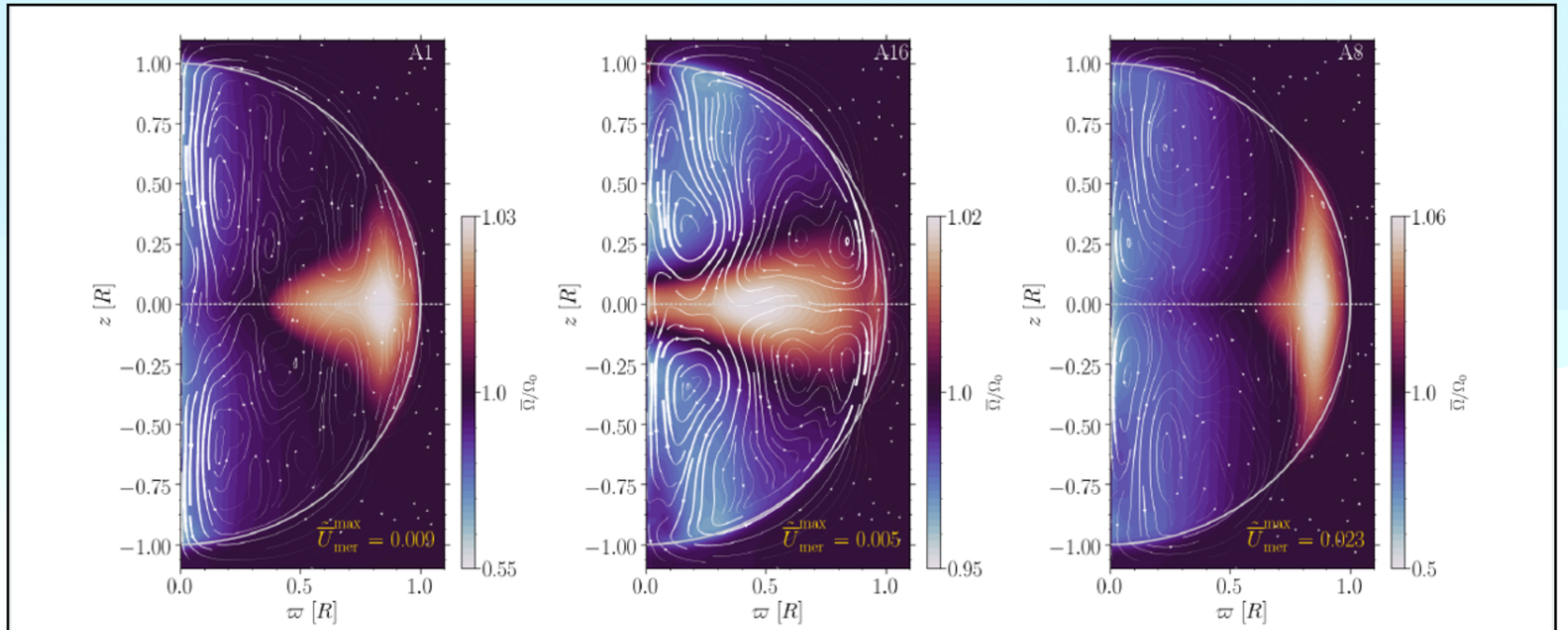

Fig. 2. Normalised time-averaged mean angular velocity $\overline{\Omega}/\Omega_0$ for simulations A1 (left), A16 (middle), and A8 (right). The coloured contours indicate $\overline{\Omega}(\varpi, z)$. The streamlines indicate the mass flux due to meridional circulation. The amplitude of the meridional flow speed ($\tilde{\overline{U}}_{\mathrm{mer}}^{\mathrm{max}}$) is indicated in the lower right corner of each panel. The surface is indicated by the grey line, while the equator is indicated by the grey dotted line.

Differential rotation is quenched at high $\mathrm{Re_M}$.

Large scale magnetic fields

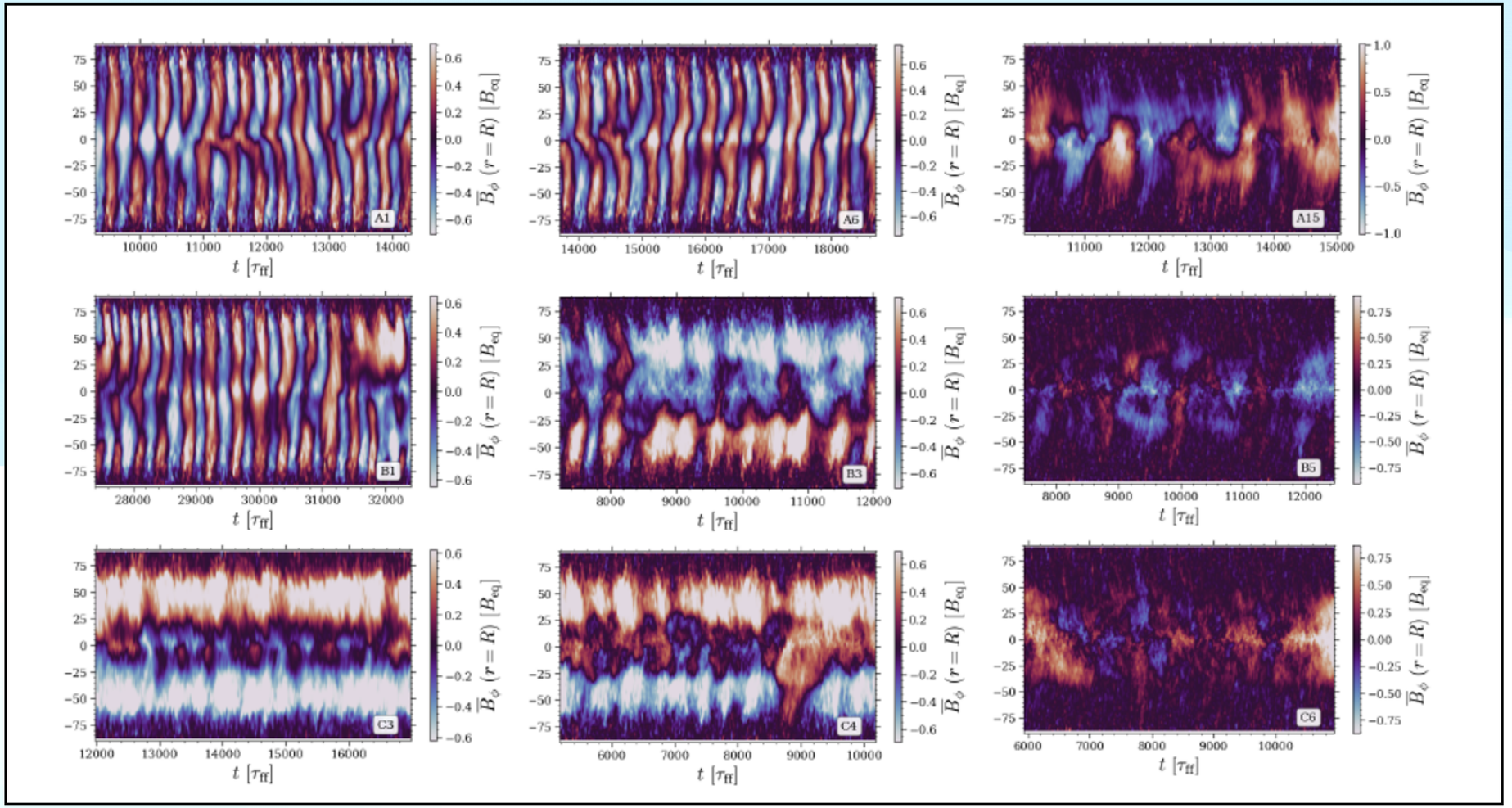

When $\mathrm{Re_M}$ is increased sufficiently, the relatively regular cycles of large-scale fields found at low and moderate $\mathrm{Re_M}$ are disrupted.

Azimuthally averaged toroidal magnetic field near the surface of the star as a function of time.

Evolved late-type stars using the star-in-a-box setup

- Magnetic fields have been observed in RGB stars.
- Chromospheric emission scales in the same way with the Rossby number in young (main sequence) and evolved (giant) late-type stars (Lehtinen, J. J.,et al. 2020, Nature Astronomy, 4(7), 658-662).
- High core-to-envelope rotation rate (Beck, P. G.,et al. 2012, *Nature*, *481*(7379), 55-57).

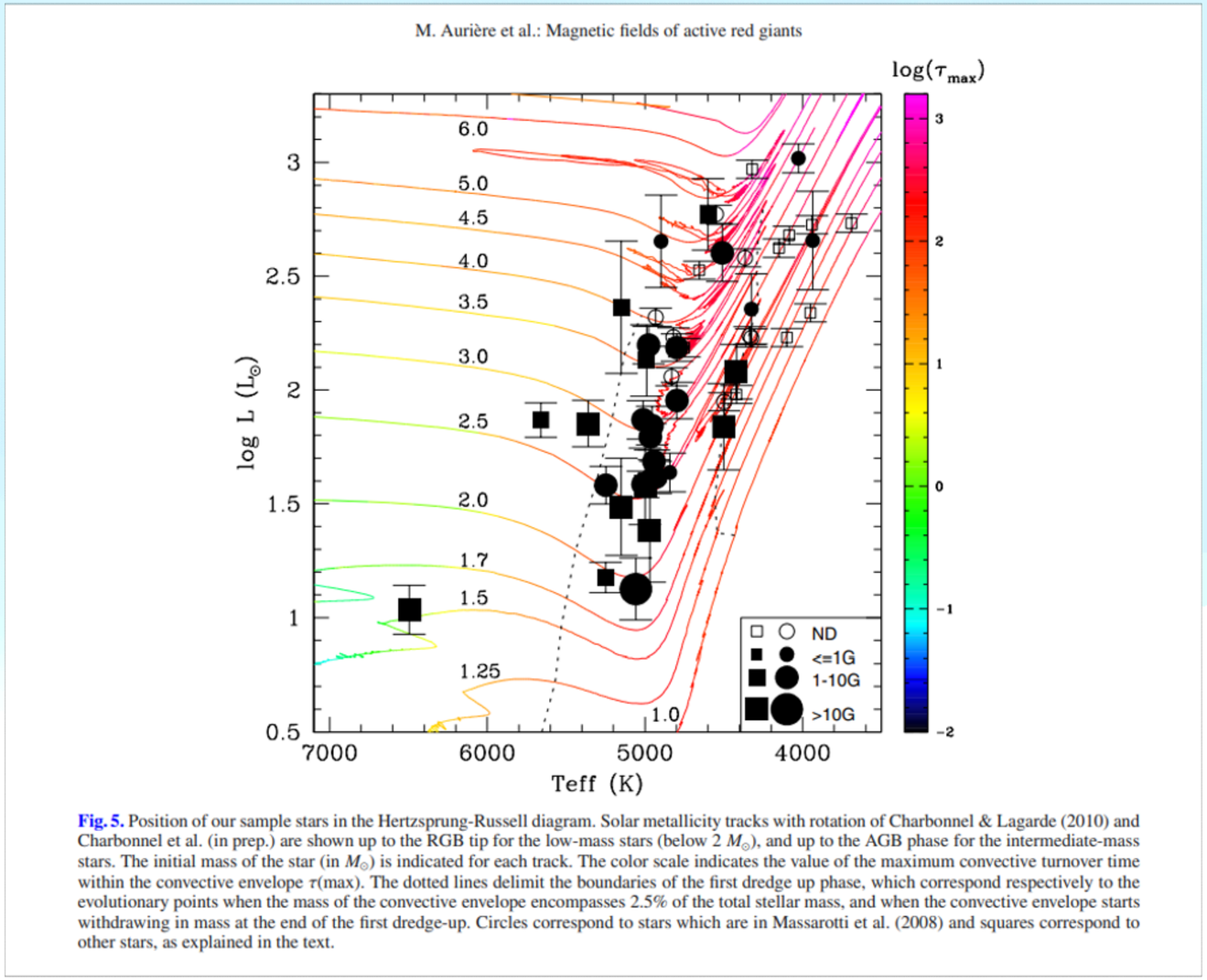

Fig. 5. Position of our sample stars in the Hertzsprung-Russell diagram. Solar metallicity tracks with rotation of Charbonnel & Lagarde (2010) and Charbonnel et al. (in prep.) are shown up to the RGB tip for the low-mass stars (below 2 $M_{\odot}$), and up to the AGB phase for the intermediate-mass stars. The initial mass of the star (in $M_{\odot}$) is indicated for each track. The color scale indicates the value of the maximum convective turnover time within the convective envelope τ(max). The dotted lines delimit the boundaries of the first dredge up phase, which correspond respectively to the evolutionary points when the mass of the convective envelope encompasses 2.5% of the total stellar mass, and when the convective envelope starts withdrawing in mass at the end of the first dredge-up. Circles correspond to stars which are in Massarotti et al. (2008) and squares correspond to other stars, as explained in the text.

Figure 5 of Aurière, M., et al. (2015), A&A, 574, A90.

Red giant star setup

Considerations

Rotation periods

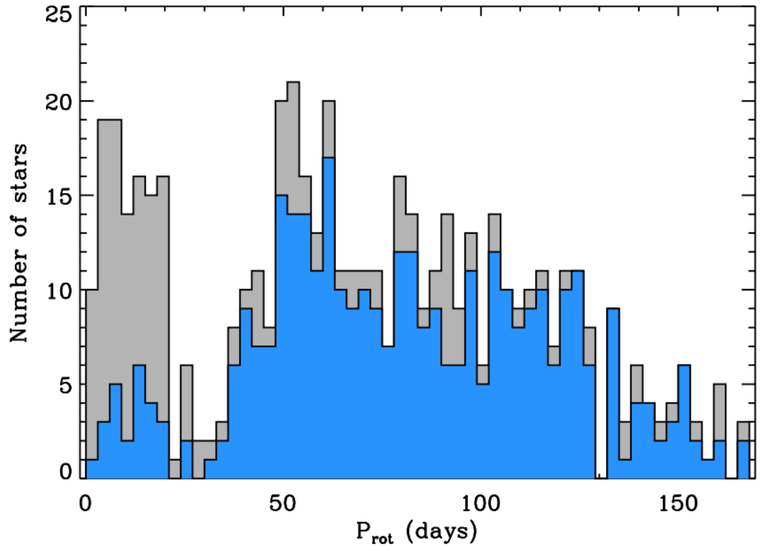

Fig. 5. Rotation periods P_{rot} for all the stars showing rotational modulation (grey, 531 stars) and for stars for which a reliable rotation period has been derived (blue, 361 stars).

Figure from Ceillier, T., et al. 2017, *A&A*, *605*, A111.

Magnetic activity

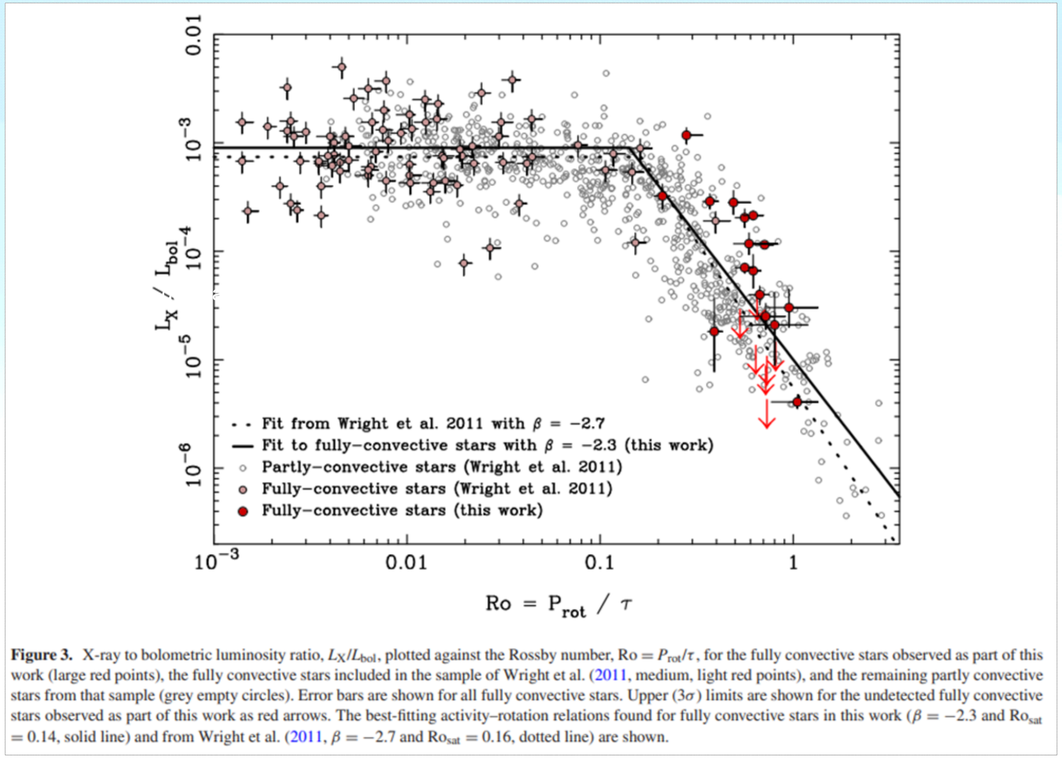

Figure 3. X-ray to bolometric luminosity ratio, L_X/L_{bol}, plotted against the Rossby number, Ro = P_{rot}/τ, for the fully convective stars observed as part of this work (large red points), the fully convective stars included in the sample of Wright et al. (2011, medium, light red points), and the remaining partly convective stars from that sample (grey empty circles). Error bars are shown for all fully convective stars. Upper (3σ) limits are shown for the undetected fully convective stars observed as part of this work as red arrows. The best-fitting activity–rotation relations found for fully convective stars in this work ($\beta = -2.3$ and Ro_{sat} = 0.14, solid line) and from Wright et al. (2011, $\beta = -2.7$ and Ro_{sat} = 0.16, dotted line) are shown.

Relation between the Rossby number and X-ray emission (normalized to the bolometric luminosity) for a sample of both fully and partially convective stars. (Wright, N. J., et al. (2018). MNRAS, 479(2), 2351-2360).

The Rossby number, Ro, measures the rotational influence on the flow.

$$Ro \sim P_{rot}/\tau_c$$

In some stars, the Rossby number is good at describing their magnetic activity.

In general, τ_c is not measured directly.

Red giant star setup

Considerations

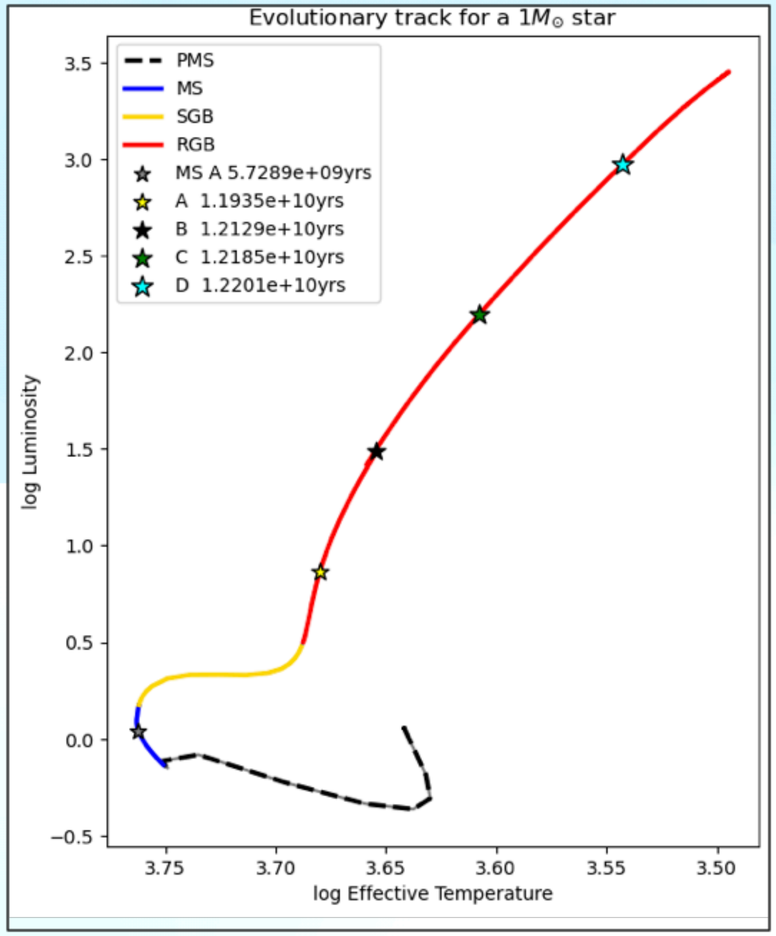

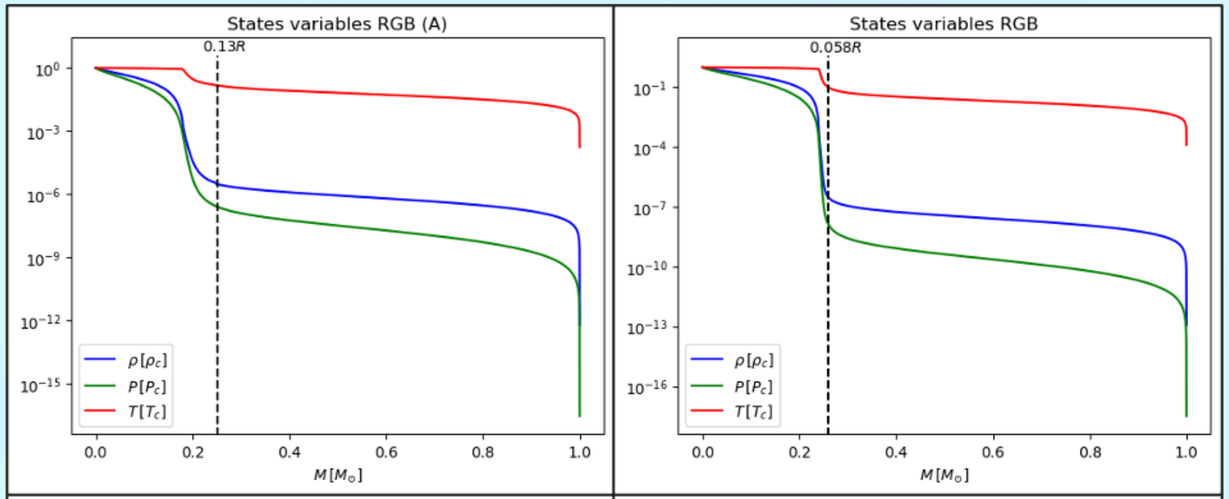

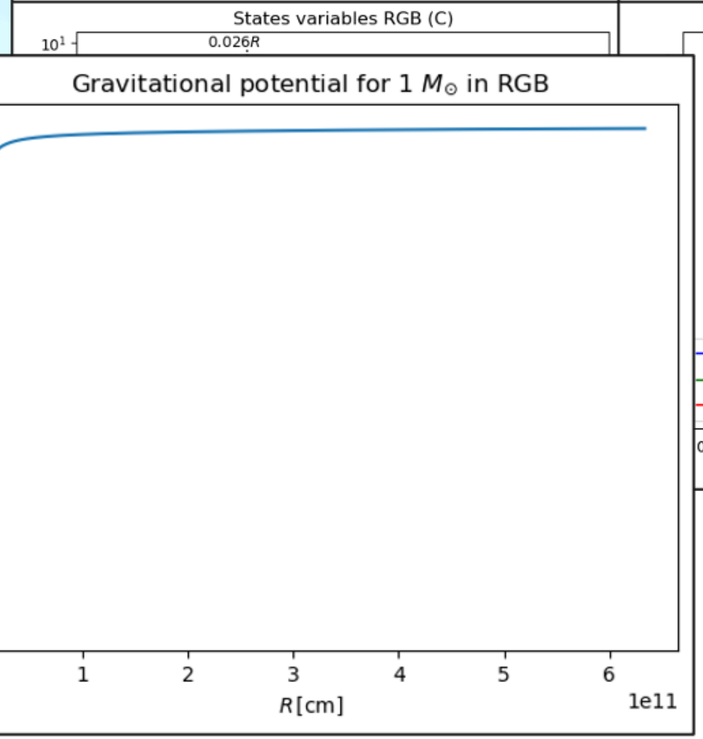

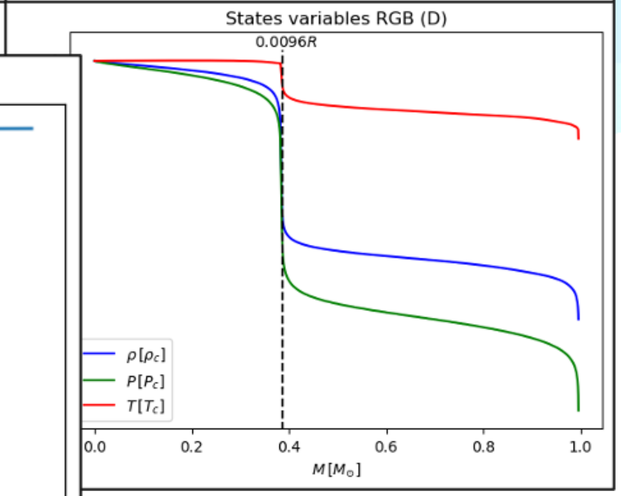

Red giant star setup

Ingredients

We need to modify and/or add:

- Gravitational potential (Freytag, B., et al. (2002). Astron. Nachr. *323*(3-4), 213-219),
- Slope-limited diffusion added for density field,
- A convective envelope by setting the value of the opacity (Kramers opacity law).

$$\Phi = -\frac{GM_*}{\left[r_0^4 + r^4/\sqrt{(1+(r/r_1)^8}\right]^{1/4}}$$

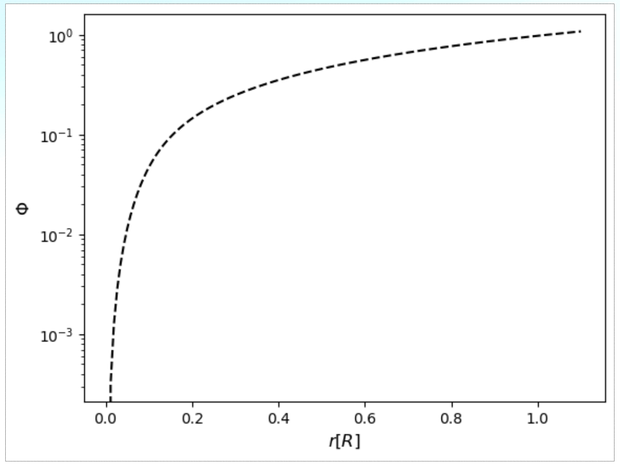

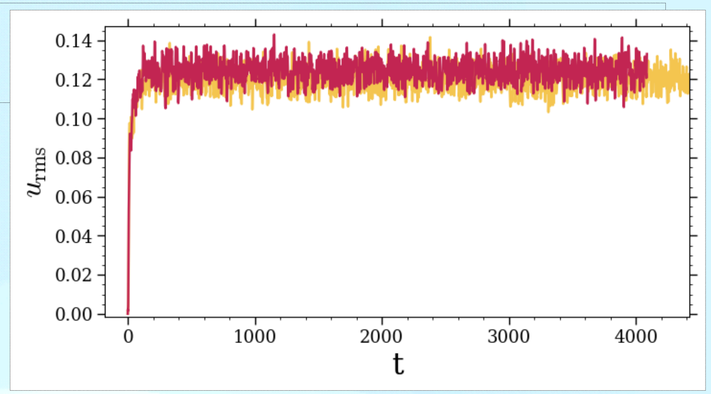

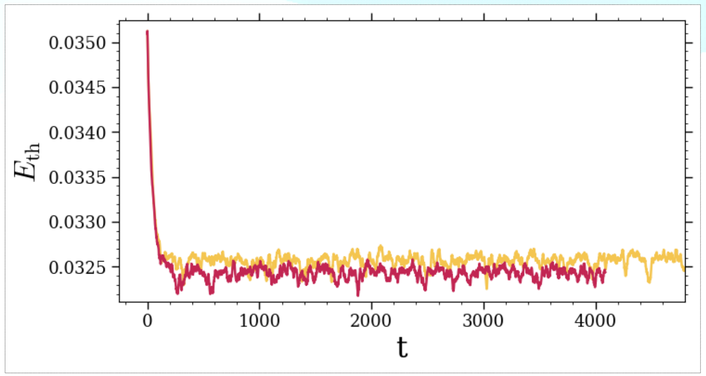

Time evolution of volumetric average thermal energy and velocity field for a run with SLD (red) and without it (yellow).

$\mathrm{Re} = 110,\ 112$
$\mathrm{Co} = 1.23,\ \ 1.25$

Red giant star setup

Preliminary results

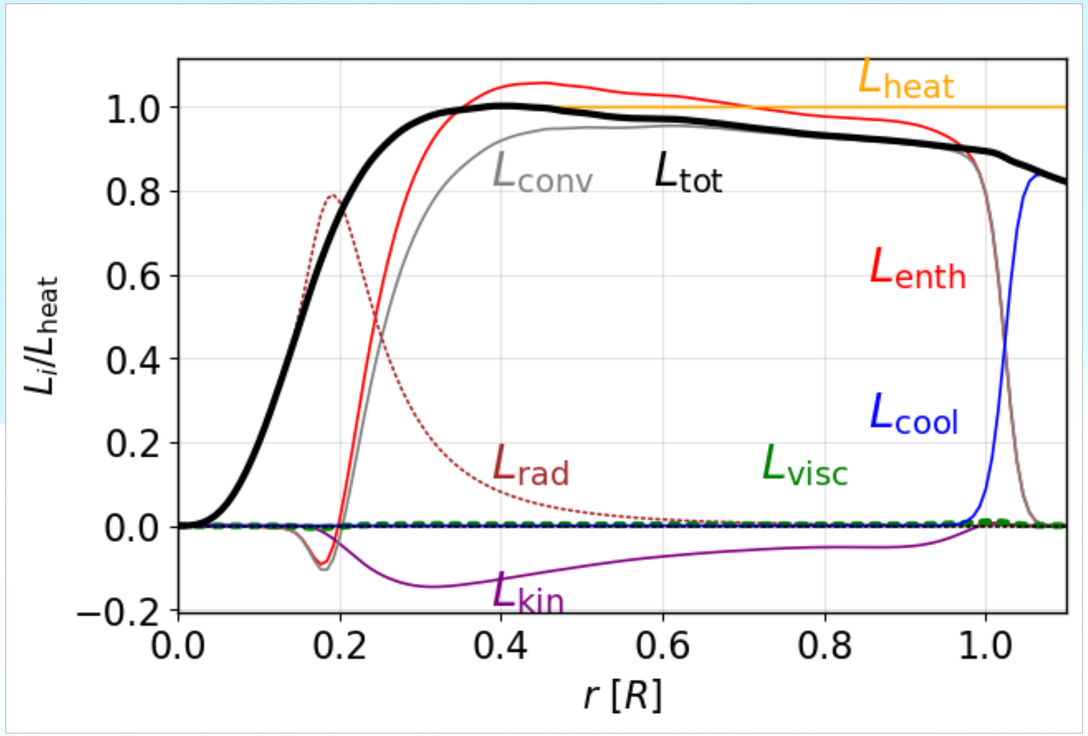

Contributions to the luminosity from enthalpy (red), kinetic energy (purple), cooling (blue), radiation (brown), convection (grey), viscosity (green) and heating (orange).

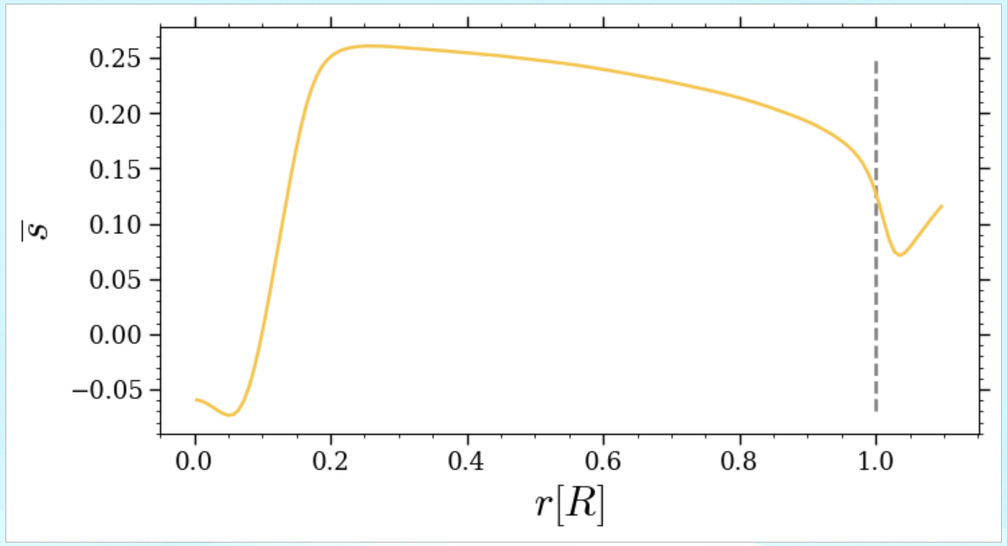

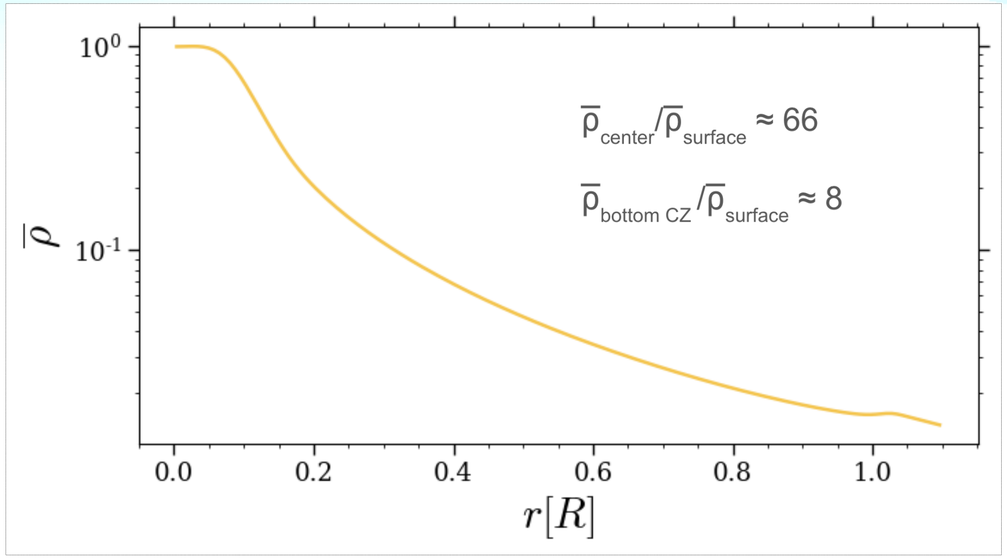

Red giant star setup

Preliminary results and next steps

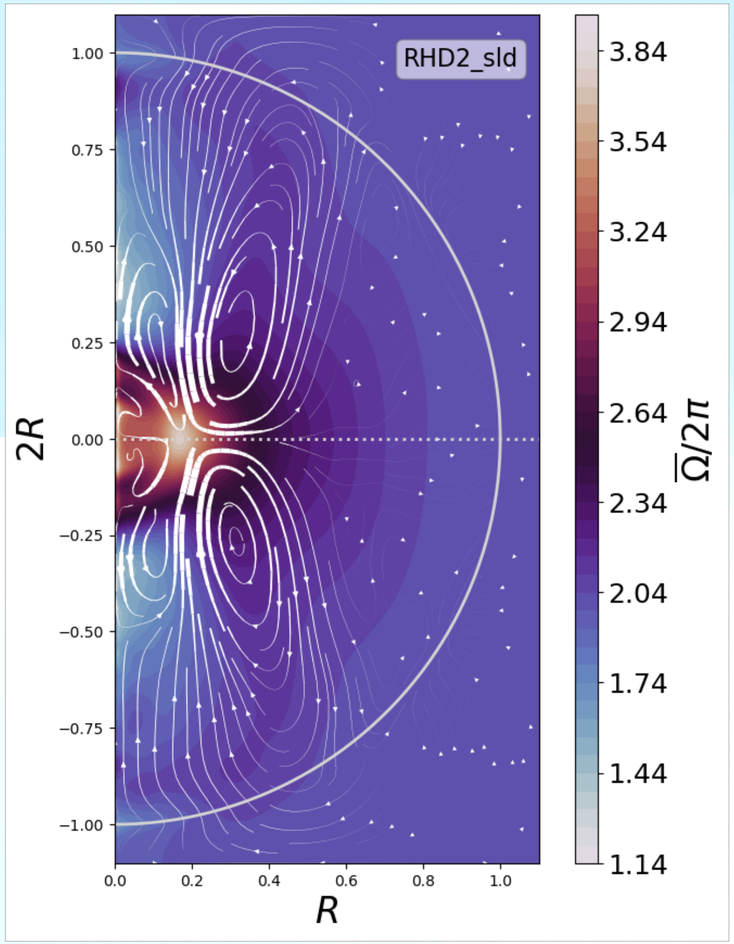

Fast core, slow envelope.
What is causing it?

$$\mathcal{T} = \varpi[\overline{\rho \boldsymbol{u} u_\phi} + \overline{\rho}\,\overline{\boldsymbol{U}}(\overline{U}_\phi + \varpi\Omega_0) - (\overline{\boldsymbol{b} b_\phi} + \overline{\boldsymbol{B}}\,\overline{B}_\phi)/\mu_0 - 2\nu\rho\overline{\mathbf{S}}\cdot\hat{\boldsymbol{\phi}}],$$

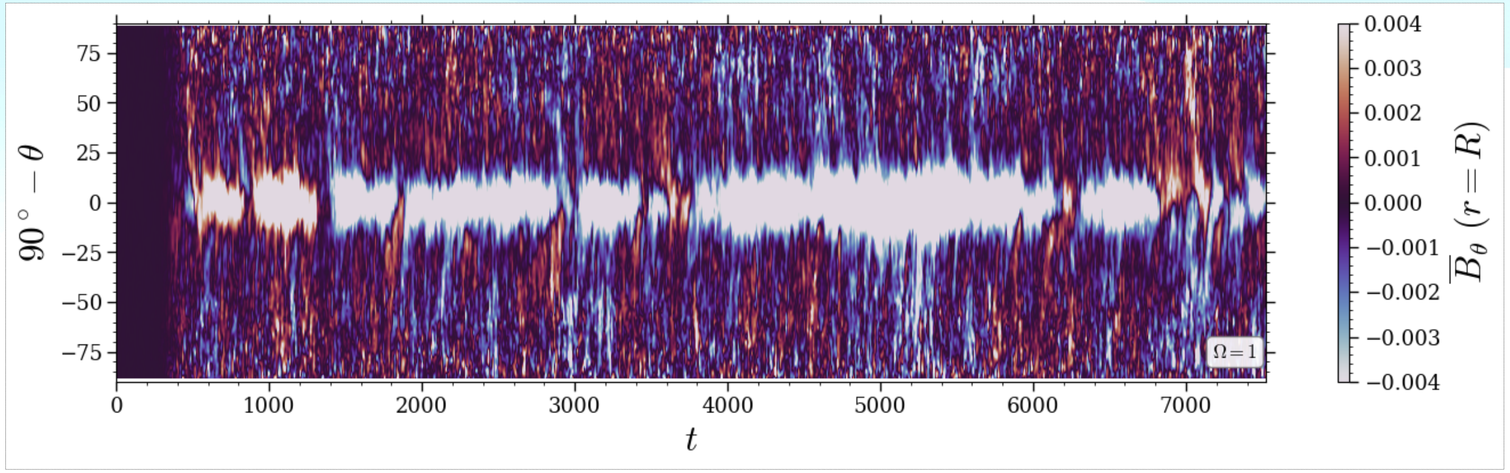

Surface magnetic fields

Red giant star setup

Next steps

- We need runs with different rotation rates. Some problems had been found,

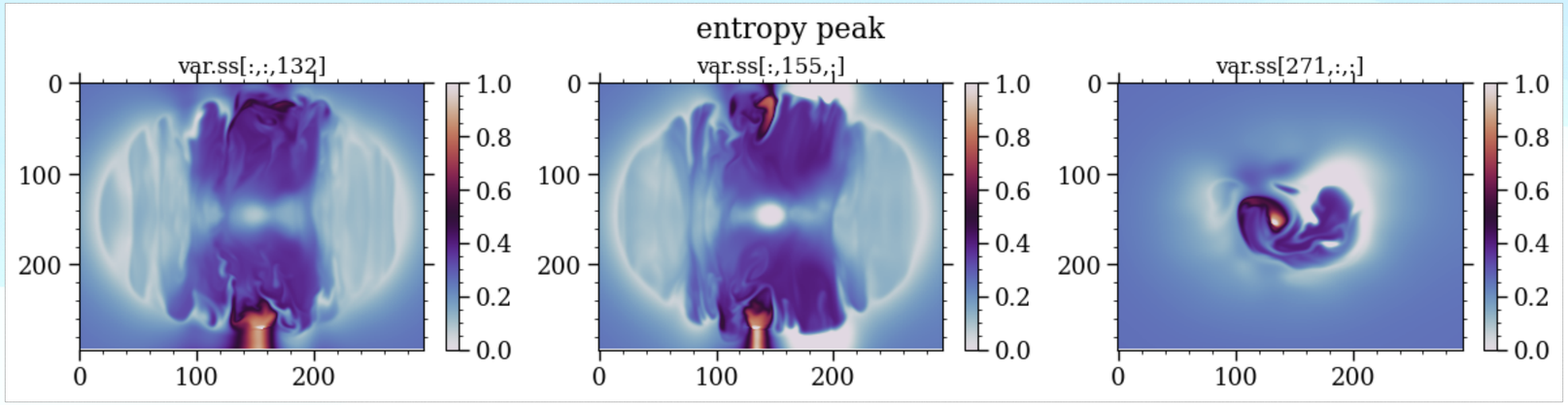

- One way to fix this may be to reduce the luminosity, $\mathscr{F} \sim u^3$.

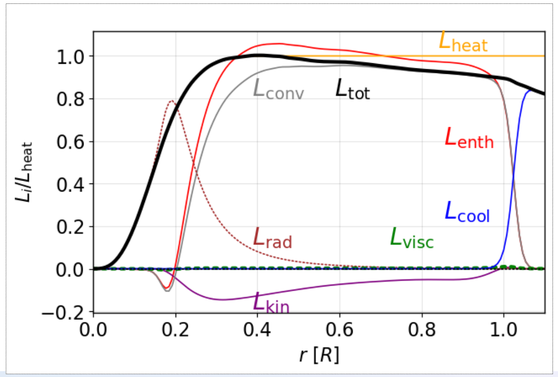

- How is the overshoot layer in these simulations?